refinement indicated that 73% of the Sn(II) atoms lie on ($2x$, x $-z$) sites together with the water (the water content was constrained to 0.74 molecules per formula unit). The remaining Sn(II) ions are on BR sites.

By comparison with the anhydrous structure, the hydrated structure is surprising. The arrangement of cations in the conduction layer is drastically altered by the intercalation of water: the favored site for the Sn(II) ion in the hydrated form becomes the asymmetric five-coordinate ($2x$, x, $-z$) site. The shortest Sn–O interatomic distance becomes 2.738 (2) Å. This closest approach of a Sn(II) ion and a water molecule is 3.125 (2) Å. This configuration occurs when both the water molecule and Sn(II) ion occupy ($2x$, x, $-z$) sites related by a center of symmetry. The water molecule thus interacts more strongly with oxygens in the spinel block than with the Sn(II) ions. A similar situation exists in hydrated Ca(II)–β''-alumina.[23] This structural information, together with the similarity of the binding energies for water in different isomorphs, suggests that the absorption of water by various β''-alumina compositions is principally the result of interaction between water molecules and the β''-alumina framework and is influenced less by cation type. A more complete description of the structure of the hydrated divalent β''-aluminas is provided elsewhere.[23]

The movement of 73% of the Sn(II) ions away from BR sites on water intercalation also explains the observed contraction of the c axis. Not only is the Sn(2)–O(3) bond shorter than in the anhydrous compound, it is also no longer parallel to the c axis. Structural rearrangements resulting from hydration may account for changes in other physical properties. Although the effect of hydration on the conductivity of the Sn(II) isomorph was not studied, the conductivity of Pb(II)–β''-alumina decreases as a result of hydration.[28] The same can be expected for the Sn(II) form.

Conclusions

Sn(II)–β''-alumina is a new luminescent solid electrolyte in the β''-alumina family of compounds. In this investigation we have characterized its synthesis, composition, structure, transport and optical properties, and most importantly, its reactivity with water. Sn(II)–β''-alumina hydrates readily, and the reaction affects both its structure and properties. We believe that Sn(II)–β''-alumina illustrates many of the complex phenomena that interact to determine the properties of the β''-alumina family of compounds. Understanding these materials requires a connected approach using many different characterization techniques. The results demonstrate some of the reasons these compounds are such intriguing and unusual inorganic materials.

Acknowledgment. This research was supported in Sweden by the National Science Research Council (NFR) and in the United States by the Office of Naval Research. Additional support by the National Science Foundation, Materials Research Laboratory Program, under Grant No. DMR-8519059 is gratefully acknowledged.

Registry No. $Sn_{0.83}Mg_{0.67}Al_{10.33}O_{17}\cdot xH_2O$, 119356-42-2; $Sn_{0.83}Mo_{0.67}Al_{10.33}O_{17}$, 119356-36-4; $Na_{0.33}Mg_{0.67}Al_{10.33}O_{17}$, 127818-91-1.

Supplementary Material Available: Listings of interatomic distances and atomic positions (77 pages); listing of structure factor amplitudes (69 pages). Ordering information given on any current masthead page.

---

[28] Rohrer, G. S.; Farrington, G. C. *J. Solid State Chem.*, in press.

Bulk and Nanostructure Group II–VI Compounds from Molecular Organometallic Precursors

J. G. Brennan,[†] T. Siegrist, P. J. Carroll, S. M. Stuczynski, P. Reynders,
L. E. Brus, and M. L. Steigerwald*

AT&T Bell Laboratories, Murray Hill, New Jersey 07974

Received February 8, 1990

We describe the preparation of the solid-state compounds ZnS, ZnSe, CdS, CdSe, CdTe, and HgTe from the corresponding $M(ER)_2$ compounds (M = Zn, Cd, Hg; E = S, Se, Te; R = n-butyl, phenyl) and/or phosphine complexes thereof. We have isolated members of two different families of phosphine complexes. In the first the bidentate phosphine 1,2-bis(diethylphosphino)ethane (DEPE) is coordinated to the $M(ER)_2$ nucleus in a 1:2 ratio, and a coordination polymer is formed. In the second the DEPE/$M(ER)_2$ ratio is unity, and a dimeric compound is formed. We show that pyrolysis of these compounds in the solid state yields the bulk solid-state compound and that pyrolysis in solution yields the same solid-state compound, but in the form of nanometer-sized particles. Nanoclusters of HgTe are similarly formed by solution-phase photolysis of $Hg(TeBu)_2$.

Introduction

Precursors to group II–VI materials have been the focus of recent synthesis efforts. This work has been motivated by the desire to prepare group II–VI materials in a variety of physical forms, notably as quantum wells or quantum dots. A number of workers have shown that $M(ER)_2$ complexes (M = Zn, Cd, Hg; E = S, Se, Te; R = organic moiety) can be converted to the related solid-state compounds,[1] but unfortunately these molecular precursors are

---

[†] Current address: Department of Chemistry, Rutgers University, P.O. Box 939, Piscataway, NJ 08855.

* Author to whom correspondence should be addressed.

[1] (a) Kern, R. J. *J. Am. Chem. Soc.* **1953**, *75*, 1865. (b) Peach, M. E. *J. Inorg. Nucl. Chem.* **1973**, *35*, 1046. (c) Peach, M. E. *J. Inorg. Nucl. Chem.* **1979**, *41*(9), 1390. (d) Osakada, K.; Yamamoto, T. *J. Chem. Soc., Chem. Commun.* **1987**, 1117. (e) Steigerwald, M. L.; Sprinkle, C. R. *J. Am. Chem. Soc.* **1987**, *109*, 7200. (f) Brennan, J. G.; Siegrist, T.; Carroll, P. J.; Stuczynski, S. M.; Brus, L. E.; Steigerwald, M. L. *J. Am. Chem. Soc.* **1989**, *111*, 4141.

0897-4756/90/2802-0403$02.50/0

rather difficult to isolate in crystalline form (and therefore difficult to purify). This is due to the complicated polymeric structure of these compounds in the solid state.[2] For example, only donor solvents such as DMF or DMSO have been reported to disrupt the polymeric network of Cd($SPh)_2$ and dissolve the compound.[3]

In this paper, we report the preparation of two families of phosphine derivatives of the $M(EPh)_2$ compounds containing the 1,2-bis(diethylphosphino)ethane (DEPE) ligand. These complexes form and crystallize readily and therefore are reliably purified. Furthermore we show that the phosphine-substituted compounds can be converted to the related solid-state metal chalcogenides and that the phosphine ligands do not interfere with this process. We show that soluble, passivated nanometer-sized clusters of cadmium telluride and mercury telluride result when the decomposition of phosphine-substituted complexes are conducted in solution. This further demonstrates that nanoclusters, as well as being of interest for their own properties, can be intermediates in reactions that take molecular precursors to solid-state materials.

Experimental Section

All reactions were performed in an inert-atmosphere glovebox or under standard Schlenk conditions, using dried, degassed solvents (Aldrich). ^1H NMR spectra (30 °C, NC_5D_5) were recorded on a GE QE-300 spectrometer. X-ray powder patterns were measured on a Rigaku Miniflex diffractometer. Transmission electron microscopy was performed on a JEOL FX2000 operating at 200 kV. Elemental analyses were performed by Schwarzkopf Microanalytical Laboratories. Melting points were measured in sealed tubes and are uncorrected. $ZnEt_2$, $CdMe_2$ (Alfa), PhSH, PhSeH, DEPE, and DMPE (Strem) were purchased and used without further purification. $Hg(TePh)_2$,[4] $Cd(SPh)_2$, $Cd(SePh)_2$, and $Cd(TePh)_2$[5] were prepared according to literature procedure.

$Zn(SPh)_2$: Thiophenol (2.4 g, 21.8 mmol) was added to diethylzinc (1.29 g, 10.8 mmol) in toluene (20 mL). There was immediate gas evolution, and a white precipitate formed. After 2 h, heptane (10 mL) was added to the mixture, and the white solid was collected by filtration and washed with heptane (10 mL). Anal. Calcd for $C_{12}H_{10}S_2Zn$: C, 50.8, H, 3.55; S, 22.6; Zn, 23.0. Found: C, 49.2; H, 3.72; S, 22.6; Zn, 23.0. ^1H NMR δ 7.84 (d, 2 H), 6.93 (t, 2 H), 6.76 (t, 1 H).

$Zn(SPh)_2$–DEPE: To $Zn(SPh)_2$ (0.21 g, 0.74 mmol) suspended in toluene (10 mL) was added DEPE (0.35 g, 1.6 mmol) and pyridine (0.5 mL). The solution was stirred for 12 h, filtered, concentrated to ca. 15 mL, and cooled (−20 °C) to give colorless diamonds (0.070 g, 19%), mp 146.8–147 °C. Anal. Calcd for $C_{22}H_{34}P_2S_2Zn$: C, 53.9; H, 6.99; P, 12.6; S, 13.1; Zn, 13.3. Found: C, 53.9; H, 6.84; P, 12.4; S, 13.4; Zn, 13.5. ^1H NMR δ 7.85 (d, 2 H), 6.93 (t, 2 H), 6.80 (t, 1 H), 1.36 (m, 2 H), 1.20 (m, 4 H), 0.89 (m, 6 H).

$Zn(SePh)_2$: Selenophenol (3.39 g, 21.6 mmol) was added to $ZnEt_2$ (1.00 g, 8.37 mmol) in toluene (20 mL). Gas evolution was immediate, and a white precipitate began to form after approximately one-fourth of the selenophenol was added. The mixture was stirred at room temperature for 6 h, after which heptane (20 mL) was added. The precipitate was collected by filtration, washed with heptane (10 mL), and dried under vacuum, to give a white solid (3.0 g, 95%), mp > 300 °C. Anal. Calcd for $C_{12}H_{10}Se_2Zn$: C, 38.2; H, 2.67; Se, 41.8; Zn, 17.3. Found: C, 39.1; H, 2.92; Se, 39.6; Zn, 18.3. ^1H NMR δ 7.91 (t, 2 H), 6.87 (m, 3 H).

$Zn(SePh)_2$–DEPE: DEPE (0.51 g, 2.5 mmol) was added to $Zn(SePh)_2$ (0.63 g, 1.7 mmol) suspended in toluene (25 mL). The mixture was stirred for 12 h, pyridine (2.8 mL) and heptane (15 mL) were added, the solution was filtered and cooled (−20 °C) to give colorless diamonds (0.63 g, 64%), mp 137.8–138 °C. Anal. Calcd for $C_{22}H_{34}P_2Se_2Zn$: C, 45.3; H, 5.87; P, 10.6; Zn, 11.2. Found: C, 45.3; H, 5.79; P, 10.4; Zn, 11.3. ^1H NMR δ 7.90 (t, 2 H), 6.86 (m, 3 H), 1.35 (m, 2 H), 1.20 (m, 4 H), 0.89 (m, 6 H).

$Cd(SPh)_2$–DEPE: DEPE (0.20 g, 0.97 mmol) was added to $Cd(SPh)_2$ (0.13 g, 0.39 mmol) in toluene (20 mL). The colorless solution was saturated with heptane (5 mL), filtered, and cooled (−10 °C) to give colorless diamonds (0.075 g, 39%), mp 129.9–131.3 °C. Anal. Calcd for $C_{22}H_{34}CdP_2S_2$: C, 49.4; H, 6.41; Cd, 21.0; P, 11.6; S, 12.0. Found: C, 49.6; H, 6.71; Cd, 21.1; P, 11.7; S, 11.7. ^1H NMR δ 7.77 (d, 2 H), 6.93 (t, 2 H), 6.80 (t, 1 H), 1.46 (m, 2 H), 1.26 (m, 4 H), 0.86 (m, 6 H).

$Cd(SePh)_2$–DEPE: DEPE (0.16 g, 0.77 mmol) was added to $Cd(SepH)_2$ (0.15 g, 0.34 mmol) in a mixture of acetonitrile (20 mL) and pyridine (0.50 mL). The solution was stirred for 2 h, filtered, and cooled (−10 °C) to give colorless diamonds (0.10 g, 45%), mp 162–164 °C. Anal. Calcd for $C_{22}H_{34}CdP_2Se_2$: C, 42.1; H, 5.41; Cd, 17.8; P, 9.78; Se, 24.9. Found: C, 43.4; H, 5.72; Cd, 17.9; P, 9.86; Se, 24.5. ^1H NMR δ 7.89 (m, 2 H), 6.88 (m, 3 H), 1.47 (m, 2 H), 1.27 (m, 4 H), 0.83 (m, 6 H).

$[Cd(SePh)_2]_2DMPE$: DMPE (0.050 g, 0.33 mmol) was added to $Cd(SePh)_2$ (0.136 g, 0.36 mmol) dissolved in pyridine (5 mL). The solution was saturated with heptane (13 mL), upon which colorless needles immediately began to precipitate. The needles (0.14 g, 75%) were collected and dried under vacuum, mp 205–7 °C. Anal. Calcd for $C_{15}H_{18}CdSe_2P$: C, 36.1; H, 3.63; P, 6.20. Found: C, 36.7; H, 3.60; P, 5.96. ^1H NMR δ 7.87 (t, 2 H), 6.87 (m, 3 H), 1.30 (m, 1 H), 0.82 (m, 3 H).

$Cd(TePh)_2$–DEPE: DEPE (0.40 g, 1.90 mmol) was added to $Cd(TePh)_2$ (0.30 g, 0.58 mmol) suspended in MeCN and pyridine (5 mL). The yellow solution was concentrated to ca. 3 mL, saturated with toluene/heptane (5:1), and cooled (−20 °C), to give yellow diamonds (0.158 g, 37%), mp 87.5–89 °C. Anal. Calcd for $C_{22}H_{34}CdP_2Te_2$: C, 36.3; H, 4.71; Cd, 15.4, P, 8.51; Te, 35.1. Found: C, 36.8; H, 4.86; Cd, 15.3; P, 8.44; Te, 34.9. ^1H NMR δ 8.04 (d, 2 H), 6.96 (m, 1 H), 6.81 (t, 2 H), 1.49 (m, 2 H), 1.30 (m, 4 H), 0.85 (m, 6 H).

$Hg(TePh)_2$–DEPE: DEPE (0.40 g, 1.94 mmol) was added to $Hg(TePh)_2$ (0.40 g, 0.67 mmol) suspended in toluene (35 mL). After stirring for 3 h, the solution was filtered, concentrated to ca. 15 mL, and cooled (−10 °C) to give yellow crystals (0.51 g, 94%), mp 95 °C (dec 128–9 °C). Anal. Calcd for $C_{22}H_{34}HgP_2Te_2$: C, 32.4; H, 4.20; Hg, 24.6; P, 7.59; Te, 31.3. Found: C, 32.7; H, 4.22; Hg, 24.4; P, 7.62; Te, 31.3. ^1H NMR δ 8.05 (d, 2 H), 6.99 (t, 1 H), 6.88 (t, 2 H), 1.62 (m, 2 H), 1.45 (m, 4 H), 0.85 (m, 6 H).

$[Hg(TePh)_2DMPE$: DMPE (0.80 g, 0.53 mmol) was added to $Hg(TePh)_2$ (0.40 g, 0.66 mmol) in pyridine (20 mL). The solution was saturated with heptane (5 mL), filtered, and cooled (−10 °C) to give yellow needles (0.22 g, 38%), mp 163.9–165.5 °C (dec). Anal. Calcd for $C_{15}H_{18}HgPTe_2$: C, 26.3; H, 2.65; Hg, 29.3; P, 4.52; Te, 37.3. Found: C, 27.3; H, 2.59; Hg, 29.6; P, 5.01; Te, 34.4. The compound was not sufficiently soluble to obtain a ^1H NMR spectrum.

$Hg(TeBu)_2$: Dibutyl ditelluride (0.62 g, 1.67 mmol) was added to a suspension of Hg (0.66 g, 3.29 mmol) in toluene/heptane (10 mL:10 mL). The mixture was allowed to stir in the dark for 16 h, while a yellow precipitate formed. The precipitate was collected by filtration, washed with heptane (5 mL), and dried under vacuum to give 0.82 g (86% based on Bu_2Te_2) of an insoluble orange–yellow solid. Anal. Calcd for $C_8H_{18}HgTe_2$: C, 16.8; H, 3.15; Hg, 35.1; Te, 44.7. Found: C, 16.6; H, 3.19; Hg, 35.0; Te, 45.3.

X-ray crystallography of $[Hg(TePh)_2DEPE]_2$: Crystal data and refinement details are summarized in Table I. Crystals, grown from toluene solutions in the presence of excess phosphine, were moderately sensitive to air and thus after examination under a polarizing microscope the samples were loaded in glass capillaries under an inert atmosphere. Data were taken on an Enraf-Nonius CAD-4 diffractometer with graphite-monochromatized Mo Kα radiation, with the NRCCAD program package. All subsequent calculations were carried out on a MicroVAX II computer running the NRCVAX crystal structure system.[6] Unit cell dimensions were

---

[2] (a) Craig, D.; Dance, I. G.; Garbutt, R. *Angew. Chem., Int. Ed. Engl.* **1986**, *25*, 165. (b) Dance, I. G.; Garbutt, R. G.; Craig, D. C.; Scudder, M. L. *Inorg. Chem.* **1987**, *26*, 4057.

[3] Barbash, Y. V.; Skrypnik, Y. G.; Shevchuk, I. A.; Korotkova, Z. G. *J. Anal. Chem. USSR (Engl. Transl.)* **1979**, *34*, 1163.

[4] (a) Okamoto, Y.; Yano, T. *J. Organomet. Chem.* **1971**, *29*, 99. (b) Dance, N. S.; Jones, C. H. W. *J. Organomet. Chem.* **1978**, *152*, 175.

[5] Stuczynski, S.; Brennan, J. G.; Steigerwald, M. L. *Inorg. Chem.* **1989**, *28*, 4431.

Table I. Crystallographic Data

compound	$[Hg(TePh)_2DEPE]_2$
empirical formula	$HgTe_2P_2C_{22}H_{34}$
formula weight	781.97
crystal system	orthorhombic
space group	*Pbca*
a, Å	16.683 (3)
b, Å	17.114 (3)
c, Å	19.187 (3)
V, Å^3	5478.1 (16)
Z	8
D_c, g/cm^3	1.896
$F(000)$	3119.47
μ(Mo Kα), mm^{-1}	7.84
cryst dimens, mm	0.20 × 0.20 × 0.20
transmission factors	0.155 054 – 0.292 055
scan type	$\theta/2\theta$
data coll	$+h+k+l$
$2\theta_{max}$, deg	49.9
cryst decay	negligible
no. of unique reflns	4813
no. of reflns with $I_{net} > 2.5\sigma(I_{net})$	1923
no. of params	135
R_f	0.052
R_w	0.035
GOF	3.246
max Δ/σ	2.483
residual density, e/Å^3	0.710

Table II. Positional Parameters and Their Estimated Standard Deviations

atom	x	y	z	B, Å^2
Hg	0.63000 (6)	0.01418 (6)	0.11949 (5)	4.69 (5)
Te(1)	0.66752 (13)	0.13855 (11)	0.03360 (12)	6.26 (10)
Te(2)	0.70818 (12)	−0.00979 (12)	0.24313 (10)	6.62 (10)
P(1)	0.6479 (6)	−0.1076 (4)	0.0445 (4)	6.5 (5)
P(2)	0.4830 (5)	0.0417 (5)	0.1487 (4)	6.8 (4)
C(1)	0.7900 (17)	0.1149 (16)	0.0139 (15)	5.8 (6)
C(2)	0.8406 (20)	0.0912 (17)	0.0629 (16)	6.7 (7)
C(3)	0.9238 (23)	0.0800 (21)	0.0527 (20)	9.0 (10)
C(4)	0.9502 (24)	0.0941 (22)	−0.0172 (22)	9.8 (10)
C(5)	0.903 (3)	0.1179 (24)	−0.0689 (22)	10.2 (11)
C(6)	0.8205 (23)	0.1252 (21)	−0.0536 (19)	8.7 (9)
C(7)	0.6851 (17)	0.0973 (17)	0.2875 (15)	6.1 (7)
C(8)	0.7131 (22)	0.1662 (21)	0.2582 (19)	8.8 (9)
C(9)	0.699 (3)	0.244 (3)	0.2863 (23)	11.6 (12)
C(10)	0.6556 (22)	0.2429 (23)	0.3503 (20)	9.0 (9)
C(11)	0.6248 (22)	0.1808 (21)	0.3768 (20)	9.1 (9)
C(12)	0.6385 (20)	0.1032 (18)	0.3511 (16)	7.4 (8)
C(13)	0.756 (3)	−0.124 (3)	0.0207 (25)	13.0 (14)
C(14)	0.8096 (25)	−0.1301 (23)	0.0803 (22)	10.7 (11)
C(15)	0.610 (3)	−0.201 (3)	0.0753 (24)	10.9 (12)
C(16)	0.608 (4)	−0.214 (3)	0.138 (3)	16.8 (20)
C(17)	0.426 (3)	−0.044 (3)	0.1899 (24)	13.1 (13)
C(18)	0.459 (3)	−0.068 (3)	0.252 (3)	13.7 (13)
C(19)	0.4622 (25)	0.1200 (24)	0.2106 (21)	11.8 (11)
C(20)	0.490 (3)	0.189 (3)	0.1865 (21)	12.6 (12)
C(21)	0.569 (3)	−0.105 (3)	−0.034 (3)	12.5 (14)
C(22)	0.404 (3)	0.057 (3)	0.0788 (23)	11.2 (12)

Table III

compound	mp	oven temp, °C	ME yield
$Zn(SPh)_2$	*a*	270	72
$Zn(SePh)_2$	*a*	270	83
$Cd(SPh)_2$	*a*	300	83
$Cd(SePh)_2$	*a*	300	97
$Cd(TePh)_2$	*a*	280	99
$Hg(TePh)_2$	*a*	120	93
$Zn(SPh)_2$–DEPE	147	270	101
$Zn(SePh)_2$–DEPE	138	270	105
$Cd(SPh)_2$–DEPE	130	350	90
$Cd(SePh)_2$–DEPE	163	300	95
$Cd(TePh)_2$–DEPE	88	250	86
$Hg(TePh)_2$–DEPE	95	280	95
$Cd(SePh)_2$–$^1/_2$DMPE	206	320	78
$Hg(TePh)_2$–$^1/_2$DMPE	164	200	86
$Cd(SePh)_2$–$^1/_2$DEPE	159	300	92

[a] These compounds decompose prior to melting.

obtained by measuring absolute 2θ values of 21 reflections in the range 35–40°. No intensity variation was noted over the course of the data accumulation. Gaussian integration absorption corrections were applied. Refinement procedures were as described elsewhere.[7] Hydrogen atoms were not included; all atoms were refined anisotropically. Final positional parameters are given in Table II. (The complex $[Cd(SePh)_2DEPE]_2$ is isostructural with lattice parameters a = 16.163 (13) Å, b = 16.737 (10) Å, and c = 19.523 (14) Å.) Positional parameters for $[Hg(TePh)_2DEPE]_2$ are included in the supplementary material (see the paragraph at the end of the paper). X-ray powder diffraction (included in the supplementary material) was used to confirm that the other complexes ($Zn(SPh)_2$·DEPE, $Zn(SePh)_2$–DEPE, $Cd(SPh)_2$–DEPE, and $Cd(SePh)_2$–DEPE were isostructural.

Pyrolyses: Samples (ca. 30 mg) were sealed in evacuated Pyrex tubes (ca. 5 mL volume) and heated for 8 h in the center of a Lindberg tube furnace. The center of the furnace was at the temperatures listed in Table III, and there was a slight gradient toward each end. Volatile materials were subsequently collected by leaving one end of the tube at room temperature. The solids were collected, weighed, and ground prior to X-ray powder diffraction analysis. Table III gives a listing of the reaction conditions and final yields of solid ME. In the solution pyrolysis of $Cd(TePh)_2DEPE$, ca. 1 mg of the complex was dissolved in 0.5 mL of 4-ethylpyridine, and the solution was heated to reflux.

Photolysis: In the dark, $Hg(TeBu)_2$ (60 mg) was dissolved in a mixture of pyridine/DEPE (1 mL, 77 mg), and equal amounts of the resulting yellow solution were placed into two vials. Both were wrapped in aluminum foil and allowed to sit for 24 h, during which time no change was observed. The foil was removed from one vial, and the room lights were turned on. Over several hours, the exposed solution turned black. Analysis by TEM showed 30–50-Å particles with clear lattice images and X-ray diffraction rings.

Results

We have prepared several complexes of the form $M(ER)_2$ (M = Zn, Cd, Hg; E = S, Se, Te; R = organic moiety) using literature methodology and, using these, constructed members of two new families of phosphine-substituted metal chalcogen complexes. In the first of these a bidentate phosphine, either DEPE (1,2-bis(diethylphosphino)ethane) or DMPE (bis(1,2-dimethylphosphino)ethane) added to $M(EPh)_2$ in a 1:2 ratio to give an organometallic coordination polymer. In the second family of compounds DEPE and $M(EPh)_2$ combine in a 1:1 ratio to give discrete molecular compounds. Each of the phosphine-substituted complexes of $M(EPh)_2$ is crystalline and has been analyzed both chemically and spectroscopically. In addition, the molecular structure of at least one member of each family has been determined crystallographically. In a recent preliminary communication[1f] we reported the structure of the polymer $[Cd(SePh)_2]_2$–DEPE. This is the representative example of the 1 phosphine:2 $M(EPh)_2$ family, and its structure is reproduced in Figure 1a. We have also determined the structure of the molecular compound $[Hg(TePh)_2$–$DEPE]_2$, the representative of the 1:1 family, and that is shown in Figure 1b. Crystal data for $[Hg(TePh)_2$–$DEPE]_2$ are given in Table I, and positional parameters in Table II. We have identified the other mem-

---

(6) (a) LePage, J.; White, P. S.; Gabe, E. J. *Proc. Am. Cryst. Assoc. Annu. Meeting, 1986*; Hamilton, Canada; AIP: New York, 1986; Poster PA23. (b) Gabe, E. J.; Lee, F. L.; LePage, J. In *Crystallographic Computing 3*; Sheldrick, G. H., Kruger, C., Goddard, R., Eds.; Clarendon: Oxford, 1985; p 163.

(7) Siegrist, T.; Schneemeyer, L.; Sunshine, S. A.; Waszczak, J. V. *Mater. Res. Bul.* **1988**, *23*, 1429.

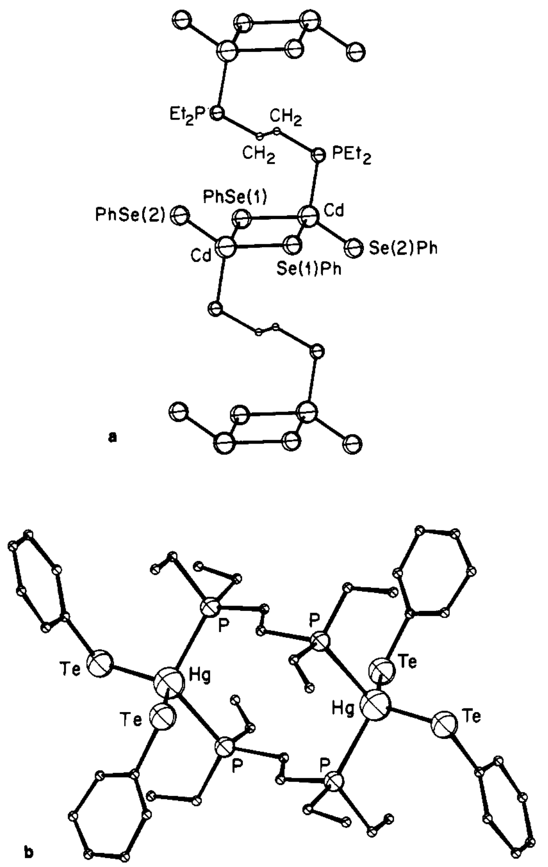

Figure 1. (a) ORTEP drawing of the backbone of [Cd(SepH)$_2$]$_2$[Et$_2$PCH$_2$CH$_2$PEt$_2$], with the phenyl and ethyl groups removed for clarity. Significant distances (Å) are as follows: Cd–Se(1), 2.735 (3); Cd–Se(1a), 2.678 (3); Cd–Se(2), 2.564 (3); Cd–P, 2.582 (7). Significant angles (deg) are as follows: Cd–Se(1)–Cd, 83.55 (9); Se(1)–Cd–Se(1a), 96.45 (10); Se(11)–Cd–Se(2), 114.02 (11); Se(1)–Cd–P, 99.59 (17); Cd–Se(1)–C(Ph), 104.2 (7); Cd–Se(2)–C(Ph), 97.5 (7). (b) ORTEP drawing of [Hg(TePh)$_2$DEPE]$_2$. Significant distances (Å) and angles (deg) are as follows: Hg–Te(1), 2.764 (2); Hg–Te(2), 2.738 (2); Hg–P(1), 2.551 (8); Hg–P(2), 2.559 (8); Te(1)–Hg–Te(2), 121.6 (1); P(1)–Hg–P(2), 112.7 (3); Te–Hg–P(av), 107.3.

bers of each family of complex by ^{1}H NMR spectroscopy, elemental analysis, and X-ray powder diffraction.

All of the phosphine complexes of M(ER)$_2$ yield the solid-state metal chalcogenides on heating in the solid state. The phosphine as well as the organic moieties are removed during the pyrolysis and the metal chalcogenides are produced in quantitative yield.

Pyrolysis of Cd(TePh)$_2$DEPE in 4-ethylpyridine results in the formation of nanometer-sized CdTe clusters, which were identified by TEM and UV–visible spectroscopy. Both wurtzite and zinc blende clusters were observed in the electron diffraction pattern.

We have prepared the alkyltellurolate complex, Hg(TeBu)$_2$. In the absence of Lewis basis phosphines this material is insoluble, similar to the phenyltellurolates; however when DEPE is added, the complex dissolves readily in pyridine, toluene, and toluene/heptane mixtures. In this case the (presumed) complexes are so soluble that we have not been able to isolate a phosphine complex of Hg(TeBu)$_2$ as a crystalline solid. Solid Hg(TeBu)$_2$ is photolyzed at room temperature by room light to give HgTe. When DEPE is used to solubilize the complex, the photolysis can be run in pyridine. In this case the initially pale yellow solution quickly darkens to black but remains homogeneous. Analysis of this black solution with transmission electron microscopy indicates the presence of small fragments (approximately 30 Å in diameter) of the solid state compound HgTe.

Discussion

Preparation and Characterization of Phosphine Complexes of M(EPh)$_2$. When Cd(SePh)$_2$ is allowed to react with 1 equiv of DEPE in toluene at room temperature, the coordination polymer [Cd(SePh)$_2$]$_2$–DEPE forms as the only isolated product. We rationalize the formation of this polymeric product by the equilibrium summarized in eq 1. The (as yet hypothetical) mononuclear complex

$$2n\{\mathrm{Cd(SePh)_2{-}DEPE}\} \rightleftarrows \{[\mathrm{Cd(SePh)_2}]_2\mathrm{DEPE}\}_n + n\mathrm{DEPE} \quad (1)$$

of the phosphine and cadmium–selenium organometallic nucleus is not stable with respect to oligomerization, and the polymer must be recrystallized from a strong donor solvent such as pyridine.

The formation of the coordination polymer is promoted when DMPE is used in place of DEPE. The higher melting point of the DMPE complex indicates a stronger lattice energy and is consistent with the expectation that the methyl groups in DMPE will allow much tighter crystal packing than will the ethyl groups in DEPE.

These polymers are interesting structures in their own right, and since they crystallize readily they represent a solution to the problem of purification that was previously mentioned. On the other hand, there are situations (see below) in which more soluble precursors are desired. This led us to search for greater solubilizing ligands and/or ligand environments.

A large excess of DEPE will dissolve Cd(SePh)$_2$ even in noncoordinating solvents such as toluene. Presumably the function of the excess ligand is to shift reaction 1 to the left, giving exclusive formation of the "monomer" species. This compound can be isolated by crystallization, a process that is often quite slow; cooled solutions of the "monomer" deposit polyhedral crystals within hours to weeks. All of the above observations and results hold true for the entire series of M(EPh)$_2$ complexes, and the determination of the crystal and molecular structure of the "monomer" Hg(TePh)$_2$–DEPE reveals the source of this unusual behavior. In the solid state, the complex is dimeric, with each bidentate phosphine bonded to two different Hg atoms, thereby forming a 10-membered ring.

The coordination geometry about the Hg atom is close to tetrahedral but is distorted in the direction of square planar with the similar ligands mutually trans. Thus the Te–Hg–Te angle is 121.6°, and the P–Hg–P angle is 112.7 (3)°, leaving the average Te–Hg–P angle at 105.6°. Bond distances are similar to previously reported values.[8]

An examination of the X-ray diffraction powder patterns of the complexes M(EPh)$_2$–DEPE, (M = Zn, E = S, Se; M = Cd, E = S, Se, Te) show them to be isostructural with the mercury complex.

It is interesting that even with a very large excess of bidentate phosphine we were not able to isolate mononuclear chelate complexes of M(EPh)$_2$. It appears that only bidentate phosphine ligands are unable to chelate a group IIB metal:[9] there are well-characterized mercury complexes with five-membered rings having two nitrogen donors[10] or one nitrogen and one phosphorus donor.[11]

---

[8] (a) Behrens, U.; Hoffman, K.; Klar, G. *Chem. Ber.* **1977**, *110*, 3672. (b) Buergi, H. B.; Fischer, E.; Kunz, R. W.; Parvez, M.; Pregosin, P. S. *Inorg. Chem.* **1982**, *21*, 1246.

[9] Aurivillius, K.; Wendel, K. *Acta Crystallogr.* **1979**, *B32*, 2941. Also see footnote 7 in ref 8b.

Thermolysis of the Precursors To Yield Group II-VI Compounds in Bulk Form. Thermolysis of $M(EPh)_2$-DEPE complexes (see Table III) leads to quantitative formation of microcrystalline ME (as monitored by X-ray powder diffraction), with evolution of Ph_2E and intact DEPE. Phosphine ligands are inert under the conditions necessary to generate ME, but such chemical inertness has limits: thermolysis of $[Cd(SePh)_2]_2$–DEPE at 470 °C gives CdSe, but a set of low-intensity X-ray powder pattern peaks matching those for $Cd_2Se_6P_2$[12] are also present. These peaks are absent in the 470 °C thermolysis of $Cd(SePh)_2$. In addition, all zinc precursors give black microcrystalline ZnE. Pure ZnS and ZnSe are white solids, and thus the ZnE prepared here contains electronically active impurities. We have seen no indication of ZnEP phases.

Decomposition temperatures are clearly dependent upon both the metal and chalcogen, with more ionic precursors requiring elevated thermolysis conditions. For the chalcogen series, this is best illustrated by the $Cd(EPh)_2$–DEPE complexes, where the decomposition temperatures are CdS (>305 °C), CdSe (250 °C), and CdTe (220 °C). Metal influences can be seen by comparing decomposition temperatures of ZnSe (>305 °C) and CdSe (250 °C) or CdTe (220 °C) and HgTe (128 °C). These reaction temperatures parallel reaction conditions necessary in traditional ceramic ME preparations.

The degree of crystallinity of the solid-state metal chalcogenide products depends significantly on the thermolysis conditions. Thermolysis of $Cd(SePh)_2$ at higher temperatures leads to the thermodynamically stable hexagonal (wurtzite) phase, but at lower temperatures the powder pattern resembles that reported for cubic (zinc blende) CdSe. This implies either that the cubic phase is formed directly and then isomerizes to the hexagonal structure or that the material initially formed is a random polytype whose powder diffraction pattern mimics that of the cubic structure.[13] Phosphine ligands also have a pronounced effect upon product crystallinity. When pyrolyzed side by side, the CdSe precursors that contain phosphine ligands give CdSe having powder pattern peak intensities that more closely resemble crystalline wurtzite CdSe, relative to the CdSe formed from $Cd(SePh)_2$ (Figure 2). The phosphine ligand is acting as a solvent, stabilizing the initially formed CdSe cluster and allowing for the elimination of lattice imperfections.

Pyrolysis in Solution To Give Nanoclusters. Nanometer-sized fragments (nanoclusters) of bulk solid-state compounds are of increasing interest in materials chemistry. Nanoclusters of semiconducting materials have been intensively studied to determine how the characteristic properties of the bulk develop with size.[14] The synthesis of these materials is difficult because of the requirement of monodispersity in both shape and size, as well as the requirement of perfect crystallinity. In most instances nanoclusters have been made by using some form of arrested precipitation reaction.[15] While very effective and simple, this approach is of limited scope, and there is therefore a strong impetus to find new and general synthesis routes to these materials. We recently reported that nanoclusters are intermediates in the solution thermolysis reaction that takes $Cd(SePh)_2$ to CdSe.[1f] In the present work we show that this route is reasonably general.

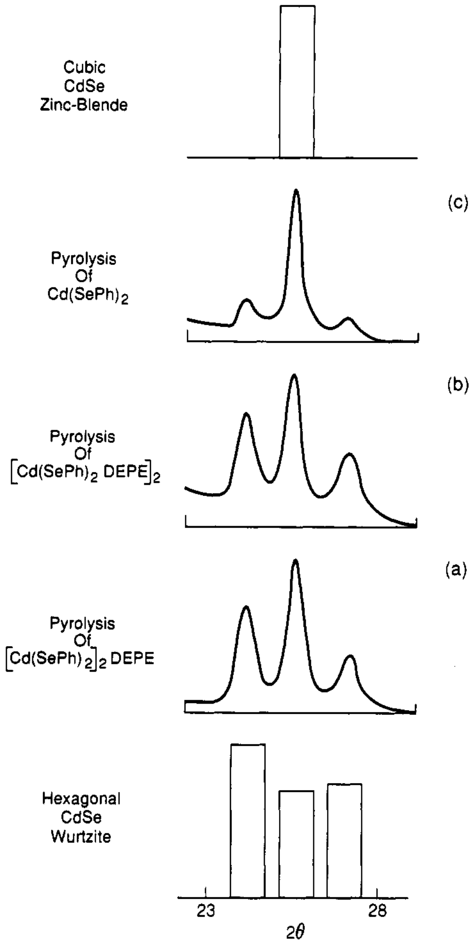

Figure 2. X-ray powder diffraction patterns of the CdSe formed via molecular thermolysis. The precursor compounds containing phosphine ligands clearly give diffraction patterns that approach that of crystalline wurtzite CdSe.

In the same way that nanoclusters of CdSe are intermediates in the solution phase thermolysis of $Cd(SePh)_2$, nanoclusters of CdTe are intermediates in the thermolysis

---

(10) (a) Cariati, F.; Ciani, G.; Menaube, L.; Pellacani, G. C.; Rassu, G.; Sironi, A. *Inorg. Chem.* **1983**, *22*, 1897. (b) Cannas, M.; Cristini, A.; Marongiu, G. *Cryst. Struct. Commun.* **1978**, *7*, 37. (c) Cannas, M.; Cristini, A.; Marongiu, G. *Inorg. Chim. Acta* **1976**, *18*, L10.

(11) Sen Gupta, P. K.; Houk, L. W.; van der Helm, D.; Hossain, M. B. *Inorg. Chim. Acta* **1980**, *44*, L235.

(12) Brec, R.; Ouvrard, G.; Louisy, A.; Rouxel, *J. Ann. Chim. Fr.* **1980**, *5*, 499.

(13) Bawendi, M.; Kortan, R.; Steigerwald, M.; Brus, L. *J. Chem. Phys.* **1989**, *91*, 7282.

(14) (a) Brus, L. E. *J. Phys. Chem.* **1986**, *90*, 255. (b) Brus, L. *Nouv. J. Chem.* **1987**, *11*, 123.

(15) (a) Rosetti, R.; Hull, R.; Gibson, J. M.; Brus, L. E. *J. Chem. Phys.* **1984**, *82*, 552. (b) Meissner, D.; Memming, R.; Kastening, B. *Chem. Phys. Lett.* **1983**, *96*, 34. (c) Mau, A. W. H.; Huang, C. B.; Kakuta, N.; Bard, A. J.; Campion, A.; Fox, M. A.; White, M. J.; Webber, S. E. *J. Am. Chem. Soc.* **1984**, *106*, 6537. (d) Kuczynski, J. P.; Milosavljevic, B. M.; Thomas, J. K. *J. Phys. Chem.* **1984**, *88*, 980. (e) Tien, H. T.; Bi, Z. C.; Tripathi, A. K. *Photochem. Photobiol.* **1986**, *44*, 779. (f) Wang, Y.; Mahler, W. *Opt. Comm.* **1987**, *61*, 233. (g) Wang, Y.; Suna, A.; Mahler, W.; Rasowski, R. *J. Chem. Phys.* **1987**, *87*, 7315. (h) Mahler, W. *Inorg. Chem.* **1988**, *27*, 435. (i) Fojtik, A.; Weller, H.; Koch, U.; Henglein, A. *Ber. Bensenges. Phys. Chem.* **1984**, *88*, 969. (j) Wang, Y.; Herron, N. *J. Phys. Chem.* **1987**, *91*, 257. (k) Zao, X. K.; Baral, S.; Rolandi, R.; Fendler, J. H. *J. Am. Chem. Soc.* **1988**, *110*, 1012. (l) Youn, H. C.; Tricot, Y.-M.; Fendler, J. H. *J. Phys. Chem.* **1985**, *89*, 1236, and references therein. (m) Meyer, M.; Wallberg, C.; Kurihara, K.; Fendler, J. H. *J. Chem. Soc., Commun.* **1984**, 90. (n) Lianos, P.; Thomas, J. K. *J. Colloid Surf. Sci.* **1986**, *117*, 505. (o) Daunhauser, T.; O'Neil, M.; Johansson, K.; Witten, D.; McLendon, G. *J. Phys. Chem.* **1986**, *90*, 6074. (p) Fendler, J. H. *Chem. Rev.* **1987**, *87*, 877. (q) Petit, C.; Pileni, M. P. *J. Phys. Chem.* **1988**, *92*, 2282. (r) Steigerwald, M. L.; Alivisatos, A. P.; Gibson, J. M.; Harris, T. D.; Kortan, R.; Muller, A. J.; Tayer, A. M.; Duncan, T. M.; Douglass, D. C.; Brus, L. E. *J. Am. Chem. Soc.* **1988**, *110*, 3046. (s) Nedeljkovic, J. M.; Nenadovic, M. T.; Micic, O. I.; Nozik, A. J. *J. Phys. Chem.* **1986**, *90*, 12. (t) Nozik, A. J.; Williams, F.; Nenadovic, M. T.; Rajh, T.; Micic, O. I. *J. Phys. Chem.* **1985**, *89*, 397.

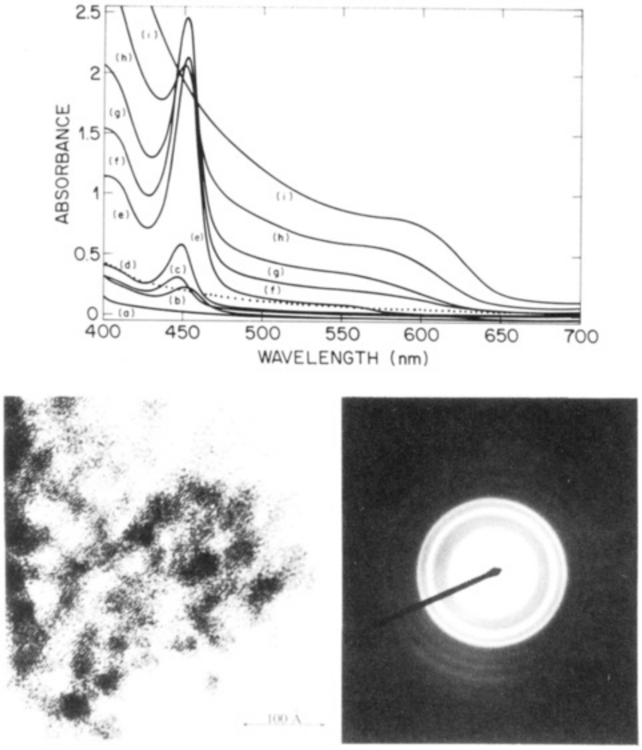

Figure 3. Top: evolution of the UV–visible absorption spectrum in the thermolysis of $[Cd(TePh)_2DEPE]_2$ (7×10^{-4} M Cd in refluxing 4-ethylpyridine). Trace a is the absorption spectrum of starting material. Traces b–f show rapid initial formation of a small CdTe cluster absorbing at 450 nm and the slower formation of larger CdTe clusters absorbing out to 600 nm. The small cluster concentration begins to decrease, as indicated in trace h, and the cluster is completely convented into larger particles by trace i. Further heating results in precipitation of all the cluster species, indicated by the dotted line. Bottom: electron micrograph of the CdTe clusters formed in solution thermolysis of $Cd(TePh)_2$–DEPE. Electron diffraction rings are consistent with the formation of CdTe particles in both the zinc blende and wurtzite modifications.

of $Cd(TePh)_2$. A comparison of the absorption spectra in Figure 3, top, to those from reference 1f shows that the two thermolyses are qualitatively similar. In the present case the molecular starting material (corresponding to trace a) is first converted to some intermediate species (yet to be identified) whose absorption spectrum peaks at 458 nm (traces b–g). This species is then converted to larger CdTe fragments as shown by the development of the "exciton" feature at approximately 610 nm. Our assignment of this absorption to nanoclusters is proven by transmission electron microscopy. In Figure 3, bottom, we show an electron micrograph of the reaction mixture directly after trace h was recorded. This micrograph shows agglomerated particles, each of which is 35–50 Å in diameter. The particles are identified as CdTe both by measuring the interplane spacing and by electron diffraction.

The electron diffraction (Figure 3, bottom) is intense and well defined and has a zinc blende pattern with an additional ring at 2.74 Å due to wurtzite CdTe. This (102) wurtzite reflection is not detectable in polytypes and does indicate here the presence of a mixture of one-phase particles.[13]

The micrographs show that the nanoclusters have agglomerated. We have not made a systematic study of this to determine at what point the fusion of particles occurs; however, the fact that the individual particles grow independently prior to fusion is clear. We have also not attempted to control the surface chemistry of the growing particles in either the CdSe or CdTe cases and therefore agglomeration (flocculation) may be expected.

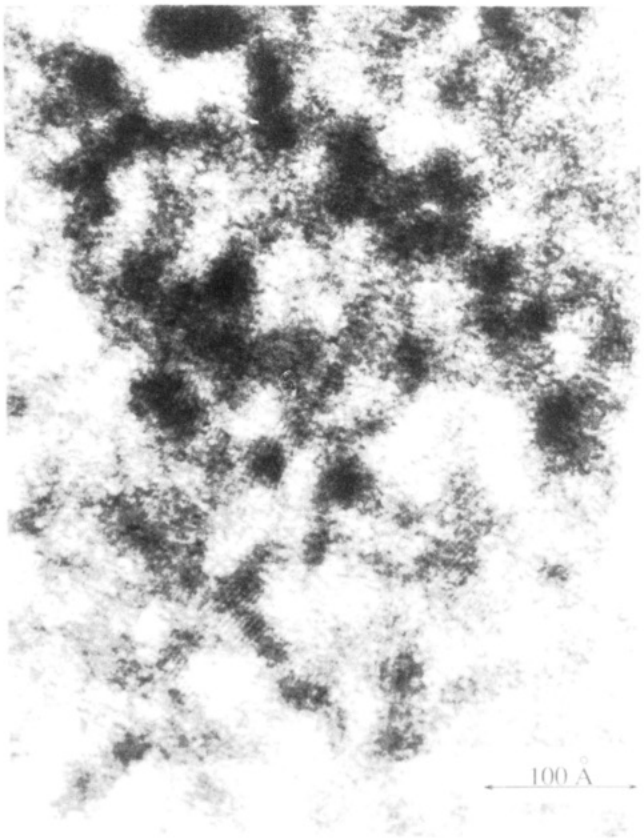

Figure 4. Electron micrograph of the HgTe particles formed in the photolysis of $Hg(Te\text{-}n\text{-}Bu)_2$.

The choice of CdSe and CdTe as the first targets of the molecular precursor synthesis of nanoclusters was convenient for two reasons. The first is that the decomposition temperatures are easily accessible and the second is that the bandgaps of the two solids are in the infrared region, and the HOMO–LUMO energy gaps in the precursors are in the ultraviolet region. These facts ensure that as the clusters grow the reactions can be followed by visible spectroscopy. By comparison, we expect that $Zn(SPh)_2$ is much too stable to form nanoclusters in 4-ethylpyridine. In any event that would be a difficult reaction to follow spectroscopically since both $Zn(SPh)_2$ and ZnS are colorless.

At the other end of the group II–VI bandgap series is HgTe. It would be valuable to determine the quantum size behavior of this semimetal, but preparation of HgTe nanoclusters by the established routes is troublesome. The molecular precursor approach should be useful since Hg compounds are much less stable than either Cd or Zn complexes. Initially, we found that gentle thermolysis of $Hg(TePh)_2$ does give HgTe, but the nanocluster stage is bypassed quickly and the solid is precipitated. We were able to circumvent this problem by replacing the phenyl groups with *n*-butyl groups.

Solutions of $Hg(Te\text{-}n\text{-}Bu)_2$ in a mixture of DEPE and pyridine are bright yellow and remain unchanged for days at room temperature in the dark. Exposure to room light for several hours gives a black apparently homogeneous solution. Absorption spectroscopy was not useful because of the absence of well-defined features throughout the process, but transmission electron microscopy was able to identify nanoclusters of HgTe in the black solution. Imaging (Figure 4) showed isolated particles ranging in size from 25 to 50 Å, and electron diffraction confirmed the presence of HgTe in the zinc blende modification.

Chem. Mater. 1990, 2, 409-415

NMR spectroscopy is a valuable tool in elucidating the internal structure and the electronic properties of semiconductor and metal clusters.[15r,16] In the case of HgTe clusters, no detectable NMR resonances or spin echoes in either ^{199}Hg and ^{125}Te NMR could be found, in contrast to the spectra of polycrystalline mercury telluride powder prepared from bulk material, which gives the expected single-line resonances in both ^{199}Hg and ^{125}Te. Experiments on CdSe clusters clearly showed resonances due to core and surface ^{77}Se atoms.[16] We attribute the lack of signal in HgTe clusters to line broadening which occurs in small particles (as was seen in the ^{77}Se NMR spectra of cadmium selenide clusters). Possible reasons for such broadening are as follows: (1) a wide chemical shift distribution due to the different chemical environments of surface and core atoms. Measurements of the precursor $Hg(TePh)_2$ ("monomeric" HgTe) in solution and in the solid state illustrate this effect: a 20% solution of $Hg(TePh)_2$ in triethylphosphine shows a narrow ^{199}Hg line (line width 120 Hz at −640 ppm relative to neat dimethylmercury). In solid-state NMR of amorphous $Hg(TePh)_2$ powder this resonances broadens to 56 000 Hz. (2) Knight shift distribution.[17] (3) Boundary-induced charge oscillations, such as those reported for lead particles smaller than 340 Å.[18]

Conclusions

We have used bidentate phosphines to isolate crystalline derivatives of the group II–VI precursor molecules $M(EPh)_2$–DEPE. These complexes can be thermally decomposed to give solid group II–VI compounds without degradation of the organic ligands. In select cases, nanometer-sized group II–VI clusters can be isolated at intermediates in the thermolysis reaction. Decomposition reactions can also be driven photolytically: $Hg(TeBu)_2$ is thermally stable at room temperature but decomposes upon exposure to room light to give first nanoclusters of HgTe and then bulk HgTe.

Acknowledgment. We are grateful to F. Padden for his assistance in learning the use of the electron microscope and to him and A. Lovinger for the use of this equipment.

Registry No. $Zn(SPh)_2$, 6865-39-0; $Zn(SePh)_2$, 120138-28-5; $Cd(SPh)_2$, 21094-83-7; $Cd(SePh)_2$, 120138-29-6; $Cd(TePh)_2$, 123676-75-5; $Hg(TePh)_2$, 97671-41-5; $[Zn(SPh)_2DEPE]_2$, 127915-92-8; $[Zn(SePh)_2DEPE]_2$, 127915-93-9; $[Cd(SPh)_2DEPE]_2$, 127915-94-0; $[Cd(SePh)_2DEPE]_2$, 127915-95-1; $[Cd(TePh)_2DEPE]_2$, 127915-96-2; $[Hg(TePh)_2DEPE]_2$, 127915-97-3; $[Cd(SePh)_2]_2DMPE$, 127915-98-4; $[Hg(TePh)_2]_2DMPE$, 127915-99-5; $[Cd(SePh)_2]_2DEPE$, 121073-86-7; ZnS, 1314-98-3; ZnSe, 1315-09-9; CdS, 1306-23-6; CdS, 1306-24-7; CdTe, 1306-25-8; HgTe, 12068-90-5.

Supplementary Material Available: Tables listing thermal parameters, significant distances and angles, and powder diffraction patterns of the molecular precursors (8 pages); table of calculated and observed structure factors (14 pages). Ordering information is given on any current masthead page.

---

[16] Thayer, A. M.; Steigerwald, M. L.; Duncan, T. M.; Douglas, D. C. *Phys. Rev. Lett.* **1988**, *60*, 2673.

[17] Townes, C. H.; Herring, C.; Knight, W. D. *Phys. Rev.* **1950**, *77*, 852.

[18] Hines, W. A.; Knight, W. D. *Phys. Rev. B* **1971**, *4*, 893.

Europium Intercalation Chemistry: Novel Behavior in TiS_2 Prepared at 500 °C

V. Cajipe, P. Molinié, A. M. Marie, and P. Colombet*

Institut de Physique et Chimie des Matériaux, CNRS-UMR 110, 2 rue de la Houssinière,
44072 Nantes Cedex 03, France

Received February 12, 1990

Eu intercalation compounds of TiS_2 prepared from the elements at 500 °C were synthesized via the liquid ammonia technique and studied by using X-ray diffraction, magnetic susceptibility measurements, and EPR. Intercalation is found to occur much more rapidly than in the case of TiS_2 prepared at higher temperatures (>600 °C); the products are also magnetically different. Data on the pristine disulfide imply that TiS_2 (500 °C) has less defects and is more stoichiometric than TiS_2 (>600 °C). This subtle distinction is proposed to account for the dramatically faster intercalation reaction and the dissimilar behavior of the resulting compounds.

Introduction

Since TiS_2 was first prepared by Berthier[1] in 1832, its existence as a stoichiometric semiconductor[2,3] and the origin of its observed metallic behavior[4-7] have been intensely disputed. Research on its numerous intercalation compounds[8] and its application as cathodes in secondary batteries[9] has likewise been vigorous. The availability of maximally stoichiometric TiS_2 has been crucial for scientific, synthetic, and technological purposes so that various procedures for its preparation have been developed.[3,10-12]

Both TiS_2 and $TiSe_2$ exhibit the CdI_2 (1T) layered structure[13] wherein the anions are hexagonally close packed and the Ti occupies half of the octahedral sites, thus

---

[1] Berthier, M. P. *Ann. Chim. Phys.* **1832**, *50*, 372.

[2] Benard, J.; Jeannin, Y. *Adv. Chem. Ser.* **1963**, *39*, 191.

[3] Thompson, A. H.; Gamble, F. R.; Symon, C. R. *Mater. Res. Bull.* **1975**, *10*, 915.

[4] McTaggart, F. K.; Wadsley, A. D. *Aust. J. Chem.* **1958**, *11*, 445.

[5] Conroy, L. E.; Park, K. C. *Inorg. Chem.* **1968**, *7*, 459.

[6] Friend, R. H.; Jérome, D.; Liang, W. Y.; Mikkelsen, J. C.; Yoffe, A. D. *J. Phys. C: Solid State Phys.* **1977**, *10*, L705.

[7] Chang, A. T.; Molinié, P.; Sienko, M. J. *J. Phys. (Paris)* **1978**, *C6*, 1070.

[8] Friend, R. H.; Yoffe, A. D. *Adv. Phys.* **1987**, *36*, 1.

[9] Whittingham, M. S. *J. Solid State Chem.* **1979**, *29*, 303.

[10] Danot, M. Thesis, Nantes, France, 1973.

[11] Thompson, A. H.; Gamble, F. R. *U.S. Patent* **1976**, 3,980,761.

[12] (a) Whittingham, M. S.; Panella, J. A. *Mater. Res. Bull.* **1981**, *16*, 37. (b) Winn, D. A.; Steele, B. C. H. *Mater. Res. Bull.* **1976**, *11*, 551.

[13] Hulliger, F. *Structural Chemistry of Layer-Type Phases*; Levy, F., Ed.; Reidel: Dordrecht, 1976; p 219.